Published in final edited form as:

Dev Cell. 2019 May 20; 49(4): 618–631.e5. doi:10.1016/j.devcel.2019.03.012.

MIR205HG is a Long Noncoding RNA that Regulates Growth Hormone and Prolactin Production in the Anterior Pituitary

Qiumei Du[1], **Ashley R. Hoover**[1,+], **Igor Dozmorov**[1], **Prithvi Raj**[1], **Shaheen Khan**[1], **Erika Molina**[1], **Tsung-Cheng Chang**[2], **M. Teresa de la Morena**[3], **Ondine B. Cleaver**[2], **Joshua T. Mendell**[2,4], **Nicolai S.C. van Oers**[1,5,6,*]

[1]Department of Immunology, The University of Texas Southwestern Medical Center, 5323 Harry Hines Boulevard, Dallas, Texas, USA 75390,

[2]Department of Molecular Biology, The University of Texas Southwestern Medical Center, 5323 Harry Hines Boulevard, Dallas, Texas, USA 75390,

[3]Department of Pediatrics, University of Washington and Seattle Children's Hospital, Seattle, WA, USA 98105

[4]Howard Hughes Medical Institute at The University of Texas Southwestern Medical Center, 5323 Harry Hines Boulevard, Dallas, Texas, USA 75390,

[5]Department of Microbiology, The University of Texas Southwestern Medical Center, 5323 Harry Hines Boulevard, Dallas, Texas, USA 75390,

[6]Department of Pediatrics, The University of Texas Southwestern Medical Center, 5323 Harry Hines Boulevard, Dallas, Texas, USA 75390,

SUMMARY

MicroRNAs (miRNAs) are processed from primary miRNA transcripts (pri-miRNAs), many of which are annotated as long noncoding RNAs (lncRNAs). We assessed whether *MIR205HG*, the host gene for miR-205, has independent functions as a lncRNA. Comparing mice with targeted deletions of *MIR205HG* and miR-205 revealed a functional role for the lncRNA in the anterior pituitary. Mice lacking *MIR205HG* had a temporal reduction in *Pit1*, growth hormone, and prolactin. This was mediated, in part, through the ability of this lncRNA to bind and regulate the transcriptional activity of Pit1 in conjunction with Zbtb20. Knockdown of *MIR205HG* in lactotropes decreased the expression of *Pit1*, *Zbtb20*, *prolactin*, and *growth hormone*, while its overexpression enhanced the levels of these transcripts. The effects of *MIR205HG* on the pituitary

[*]Lead Contact: Dr. Nicolai S.C. van Oers, NA2.200, 6000 Harry Hines Blvd., The Department of Immunology, UT Southwestern Medical Center, Dallas, TX, USA 75390-9093, Nicolai.vanoers@utsouthwestern.edu.

[+]current address: University of Central Oklahoma, 100 N. University Drive, Edmond, OK, USA 73034

AUTHOR CONTRIBUTIONS

Q.D., A.L.H., M.T.d.l.M., and N.S.C.v.O. conceived the experiments. Q.D., A.R.H., I.D., P.R., S.K., E.M., and N.S.C.v.O. performed the experiments. Q.D., A.L.H, M.T.d.l.M., and N.S.C.v.O. conceived the experiments. I.D., P.R., and S.K. analyzed the RNA Seq and array data. Q.D., A.R.H., I.D., T-S.C., M.T.d.l.M., O.B.C., J.T.M., and N.S.C.v.O. analyzed the data. Q.D. and N.S.C.v.O. wrote the manuscript. J.T.M. reviewed the manuscript.

DECLARATION OF INTERESTS

J.T.M. is on the scientific advisory board of a company called Ribometrix, which makes small molecules that target RNAs. There is no direct relationship between his role with the company and the work described in the current manuscript.

were independent of miR-205. The data support a role for *MIR205HG* as a lncRNA that regulates growth hormone and prolactin production in the anterior pituitary.

Keywords

miR-205; MIR205HG; pituitary gland; thymus; pituitary transcriptome; endocrine hormones

INTRODUCTION

Long noncoding RNAs (lncRNAs) are receiving increasing attention for their emerging roles in various physiological and developmental processes. Broadly defined as RNAs with lengths >200 nucleotides that have no protein coding potential, these lncRNAs number in the tens of thousands (Kopp and Mendell, 2018; Yang et al., 2014). Of the lncRNAs characterized to date, most exhibit limited evolutionary sequence conservation, are usually expressed at lower levels than protein coding genes, and have diverse activities (Kopp and Mendell, 2018; Quinn and Chang, 2016; Ulitsky et al., 2011). A few well-characterized lncRNAs, such as *Xist*, *HOTAIR*, *MALAT1*, and *NORAD*, each exhibit distinct functions, acting as either scaffold RNAs, transcriptional assembly hubs, regulators of chromatin accessibility, and/or controlling genome stability (Angrand et al., 2015; Lee et al., 2016; Quinn and Chang, 2016).

Several lncRNAs can also function as host transcripts for microRNAs (miRNAs). *LincMD1*, a muscle specific lncRNA, contains two miRNAs, miR-206 which is situated within an intron, and miR-133, located in a distal exon (Cesana et al., 2011). *LincMD1* regulates the timing of muscle differentiation by binding and neutralizing miR-133, which targets mRNAs involved in muscle specification. *H19* is an abundantly transcribed lncRNA present in both the fetus and pregnant mother and becomes strongly repressed at birth. This lncRNA antagonizes a methyl-transferase inhibitor, thereby increasing DNA methylation to control gene expression (Zhou et al., 2015). *H19* is also the host gene for miR-675, which is embedded within its first exon (Dey et al., 2014; Keniry et al., 2012). MiR-675 promotes muscle cell differentiation by targeting specific mRNAs for degradation (Dey et al., 2014).

MIR205HG is a noncoding RNA that acts as the host gene for miR-205, a miRNA predominantly expressed in the epithelial cells of the skin, thymus, and bladder (Farmer et al., 2013; Hoover et al., 2016; Park et al., 2012; Wang et al., 2013). The precursor of human miR-205 (pre-miR-205) spans an intron-exon boundary in the *MIR205HG* host gene, indicating that alternatively spliced isoforms of *MIR205HG* exist that do not encode the miRNA (Chang et al., 2015). Nevertheless, while MIR205HG transcripts lacking miR-205 can be formed, there are no independent functions ascribed to these. Current annotations suggest that the murine pri-miR-205 sequence resides within the distal end of the second exon of the host gene (*4631405K08Rik*). A complete knockout of miR-205 causes a failure of hair follicle regeneration in mice, an absence of lacrimal glands, and some post-natal lethality (Farmer et al., 2017; Farmer et al., 2013; Park et al., 2012; Wang et al., 2013). The selective deletion of miR-205 in thymic epithelial cells (TECs) in mice results in a thymic hypoplasia, a phenotype most obvious following stress (Hoover et al., 2016).

Validated mRNA targets of miR-205 in skin epithelial cells include negative regulators of the PI3K pathway and the Zeb1 and Zeb2 transcription factors that promote epithelial-to-mesenchymal transitions (Gregory et al., 2008; Wang et al., 2013). MiR-205 positively regulates the expression of the Foxn1 transcription factor in TECs (Hoover et al., 2016). MiR-205 also targets the p53 homolog, ΔNp63, which itself positively regulates miR-205 expression, revealing a regulatory feedback loop (De Cola et al., 2015; Tran et al., 2013; Tucci et al., 2012). MiR-205 is reported to both positively and negatively contribute to tumor initiation and progression, dependent on the cancer type (Qin et al., 2013).

Most published studies pertaining to miR-205 were undertaken without an assessment as to whether MIR205HG could function as a lncRNA independent of the miRNA. While both the host transcript and the miRNA are co-expressed in tissues that comprise epithelial cells, we report that *MIR205HG* is also transcribed in the anterior pituitary. We developed a *MIR205HG* conditional knockout mouse line and compared this with the previously developed miR-205-deficient mice. The complete loss of *MIR205HG* causes a temporal reduction of growth hormone and prolactin production in the anterior pituitary. Mechanistic studies suggest that *MIR205HG* regulates *Pou Class 1 Homeobox 1* (*Pou1f1*, also designated as *Pit1* and *Pit-1)* and *Zinc-finger and BTB-domain 20* (*Zbtb20)*, two transcription factors that control the expression of prolactin and growth hormone in lactotropes and somatotropes, respectively (Andersen and Rosenfeld, 2001; Cao et al., 2016; Kelberman et al., 2009). These processes are independent of miR-205, evidenced by a CRISPR/Cas9 knock-in mouse wherein the seed sequence specificity of miR-205 was eliminated, as well as the use of antagomirs against this miRNA in a rat lactotrope cell line. The contribution of *MIR205HG* as a lncRNA is further supported by comparative gene expression results with the pituitary versus skin tissues. Our findings support dual functions for *MIR205HG*, as a lncRNA in the anterior pituitary, and as the host gene for miR-205 in epithelial cells such as those in the thymus.

RESULTS

The Murine Host Gene for miR-205, *MIR205HG*, Comprises Multiple Transcripts in Epithelial Tissues

MiR-205 is a highly conserved epithelial-specific miRNA present in most eutherian species (Figure 1A and S1A). Human miR-205 lies within the intron-exon splice junction of an 11-exon host gene termed *MIR205HG* (1q32.2) (Figure S1B) (Chang et al., 2015). Current annotations of the murine host gene for miR-205 suggest the existence of a 2.1 kb transcript on chromosome 1 derived from 2 exons (lncRNA, *4631405K08Rik*) (Figure 1A). Nucleotide sequence comparisons of *MIR205HG* revealed considerable segmental homologies in diverse species, suggesting partial conservation of this lncRNA (Figure S1C).

The tissue tropism of murine *MIR205HG* was assessed by RT-PCR. Multiple *MIR205HG* transcripts were detected in the skin, thymus, pituitary, and bladder (Figure 1B). Transcripts were not seen in the liver, heart, spleen, hypothalamus, or lung, while very weak signals were noted in the kidney and brain (Figures 1B, 2A and S2A). Consistent with the epithelial selective expression of this lncRNA in the thymus, no transcripts were present in thymocytes, macrophages, dendritic cells, or fibroblasts (Figure S2B). Using primers distal

to miR-205 revealed transcripts about 800 nucleotides beyond the currently defined 3' end of the host gene (Figure S2C). Deep sequencing was performed on RNA prepared from the skin and thymus to confirm this. RNA-seq reads from both the skin and thymus were present throughout a 4-kb region of *MIR205HG* (Figure S2D and S2E). The read-depth with thymic RNA was less than the skin, with a read pile-up just past miR-205 (Figure S2E).

The presence of multiple *MIR205HG* transcripts in the adult pituitary tissue is unexpected as miR-205 is reportedly not expressed at this site (Bak et al., 2008; Ludwig et al., 2016). To re-assess this, RT-PCR was performed with pituitary RNA, using primers spanning different segments of MIR205HG. Transcripts comprising exon 1, exon 2, a spliced derivative of exon 1 and 2, and a longer RNA species that spans the entire intron were found (Figure 1C). These transcripts were only detected when using reverse transcriptase, ruling out genomic DNA as a contaminating source for the signals (Figure 1C, lane 3 versus lane 4). The diverse transcripts from the skin, thymus, pituitary and bladder were cloned and sequenced to assemble a complete transcript annotation for murine *MIR205HG*. Five distinct transcripts were identified (Figure 1D). The longest is 3.8 kb, extending from exon 1, through the intron, and 762 bases past the currently defined exon 2 (Figure 1D). In two of the transcripts, the pre-mature miR-205 sequence is in an intron, similar to that reported for hsa-miR-205 (Figures 1D and S1B) (Chang et al., 2015).

Differential Expression of *MIR205HG* and miR-205 in the Pituitary Gland

To compare the expression levels of *MIR205HG* relative to miR-205, particularly in the pituitary tissue, quantitative RT-PCR was used to quantitate *MIR205HG* expression. MIR205HG transcripts, detected with primers spanning the full-length host gene (Probes 1–4) were highest in the skin and bladder, followed by the thymus and pituitary tissue, were barely detected in the liver, and below detection limits in the hypothalamus (Figure 2A). These findings demonstrate that *MIR205HG* transcripts are selectively expressed in particular tissues. The miRNA levels were quantitated with the miRCURY LNA™ miRNA RT-PCR assay. Using miR-205 specific primers, the skin was found to contain the highest levels of this miRNA, followed by the bladder and thymus. In contrast, miR-205 was only marginally expressed in the pituitary tissue, with Ct values near the detection limits as defined by the samples from the liver and hypothalamus, with the liver considered a negative for this miRNA (Figure 2B). Contrasting miR-205, miR-7 was expressed at similar levels in the pituitary tissue and liver, while miR-26b was detected at equivalent levels in thymus, bladder, and hypothalamus, with none seen in the pituitary (Figure 2B). These data indicate that the lncRNA, *MIR205HG*, is produced in the pituitary tissue, which can generate miRNAs but minimal amounts of miR-205 relative to the transcript levels of the host gene.

MIR205HG is Expressed in the Region that Specifies the Anterior Pituitary during Embryogenesis

MiR-205 is expressed in embryonic tissues, as reported with LacZ reporter mice (Farmer et al., 2017; Farmer et al., 2013; Park et al., 2012). To assess the spatiotemporal expression patterns of the host gene in embryos, *in situ* hybridizations were performed with a 1.3 kb antisense probe specific for *MIR205HG*. Transcripts were detected in the

pharyngeal apparatus, limb buds, nasal process, and in the brain in e9.5-e11.5 murine embryos (Figure 2C). No expression was detected prior to e9.0 (data not shown). At e11.5, *MIR205HG* was prominent throughout the 3rd pharyngeal pouch, which contains the ventrally positioned thymic anlage (defined by *Foxn1*), and the dorsally located region that forms the parathyroid, revealed with a *Gcm2*-specific antisense probe (Figure 2D). The developing thymus contained some of the highest levels of *MIR205HG*, as revealed in cardiothoracic sections that include the thymus, or with thymic lobes from e12.5, e14.5, and e18.5 embryos (Figure S3A–B). *MIR205HG* was also expressed in Rathke's pouch (demarcated by *Pitx2*), which forms the anterior pituitary gland (Figure 2E). Other sites of expression include the olfactory nasal pit, duodenum lumen, lung buds, stomach, midgut, and pancreatic primordium (Figure S3C–L).

MIR205HG Regulates Growth Hormone and Prolactin Production

The presence of multiple *MIR205HG* transcripts in the anterior pituitary with marginal production of miR-205 could indicate an independent functional role for *MIR205HG* as a lncRNA. Multiple algorithms analyzing the coding potential of the *MIR205HG* transcripts were unable to identify regions comprising proteins, peptides, or micropeptides, further supporting a putative function for *MIR205HG* as a lncRNA (Table S1). *MIR205HG* conditional knockout mice were generated and compared with the previously described miR-205-targeted line to address the role of each noncoding RNA (Farmer et al., 2017; Farmer et al., 2013; Park et al., 2012; Wang et al., 2013). The *MIR205HG* locus was modified by incorporating loxP sites upstream of the first exon and 5' to the pre-mature miR-205 sequence (Figure 3A). This targeting construct was designed to keep miR-205 sequences intact while removing 2.5 kb of the lncRNA. The miR-205 conditional knockout allele had loxP sites upstream of miR-205 and following exon 2 (Figure 3A) (Farmer et al., 2013; Park et al., 2012; Wang et al., 2013). Cre-mediated deletion of the miR-205 targeted allele eliminates this miRNA along with 1 kb of the surrounding lncRNA (Figure 3A).

Complete knockouts of murine *MIR205HG* and miR-205 were generated by mating the floxed mice with a CAG-Cre recombinase driver line, where Cre is active in oocytes (Park et al., 2012; Sakai and Miyazaki, 1997). This targeting design eliminated *MIR205HG* transcripts (Figure S4A). The $MIR205HG^{-/-}$ offspring were smaller than either littermate controls or those with a miR-205-deficiency (Figure 3B). These size differences were seen in young mice (Figure 3C). The targeting of *MIR205HG* did not affect the expression of genes several hundred kb up- and down- stream of this region, indicating that targeting this lncRNA locus did not affect gene expression in *cis*, but did impact miR-205 (Figure S4B–C).

A possible explanation for the smaller size of the *MIR205HG* null mice was reduced levels of endocrine hormones such as growth hormone and prolactin that are produced by the anterior pituitary (Horseman et al., 1997; Perez-Castro et al., 2012; Zhu et al., 2007). In comparing post-natal day 14 mice (P14), growth hormone levels were significantly reduced in the absence of *MIR205HG* (Figure 3D). Given these reduced protein levels, we next assessed the transcript levels of *Pit1, Zbtb20*, *prolactin*, and *growth hormone*. Pit1 is a transcription factor that positively regulates prolactin, growth hormone, thyroid stimulating

hormone, and growth hormone stimulating hormone receptor expression in the anterior pituitary (Andersen and Rosenfeld, 2001; Kelberman et al., 2009). *Zbtb20* transcriptionally regulates prolactin production in lactotropes in conjunction with *Pit1* (Cao et al., 2016). Quantitative RT-PCR revealed reduced transcripts levels for *Pit1*, *Zbtb20*, *prolactin* and *growth hormone* in both P14 and P28 mice lacking *MIR205HG* (Figures 3E–F). Prolactin protein was not detectable in the serum at P14 or P28, as the levels of this protein are extremely low in young mice. Consequently, we compared the levels of prolactin in mice 5-weeks of age and older. *MIR205HG*-null female mice had a significant reduction in serum prolactin (Figure 4A). Prolactin levels were also diminished in female mice and nursing mothers from the *MIR205HG*$^{-/-}$ and miR-205$^{-/-}$ mice when compared with controls, with miR-205 null less dramatically affected (Figure 4A). While male mice produce much less prolactin than females, the levels of this hormone were also slightly reduced in the knockout mice compared to controls (Figure 4A). Among offspring from *MIR205HG*$^{+/-}$ heterozygous breeding pairs, the *MIR205HG*$^{-/-}$ mice produced less prolactin than *MIR205HG*$^{+/+}$ and *MIR205HG*$^{+/-}$ littermates (Figure 4A).

Since other endocrine- or non-endocrine dependent pathways could have been impacted by the loss of *MIR205HG* leading to the delayed growth stature, we performed blood and tissue comparisons. There were no statistically significant differences in serum corticosterone values, with this steroid regulated by adrenal corticotropin hormone (ACTH) released by the pituitary gland (Figure S5A) (Gong et al., 2015). *MIR205HG* is highly expressed in the parathyroids, which could impact growth. However, calcium, magnesium, phosphate, and potassium levels were normal, ruling out a global defect in parathyroid functions (Figure S5B). In addition, cholesterol, triglycerides, creatine kinase, and blood glucose levels were comparable (Figure S5C). While the size of the thymus was slightly reduced in the *MIR205HG* null mice, T cell development was normal (Figure S5D–E). Taken together, the data strongly suggests that *MIR205HG* regulates growth hormone and prolactin production during early post-natal development. The recovery of growth hormone production in MIR205HG$^{-/-}$ mice by 5-weeks of age likely explains the transient small stature phenotype (LaPensee et al., 2006).

MiR-205 Knock-in Mice Express Normal Levels of Pit1, Zbtb20, and Growth Hormone

The reduced levels of growth hormone and prolactin in both the *MIR205HG*- and miR-205-knockout lines leaves open the possibility that the miRNA could contribute to endocrine hormone production. For example, miR-205 was no longer detected in the *MIR205HG*-knockout line, presumably due to the elimination of regulatory elements controlling this miRNA (Figures 4B and S4C). The coupled regulation of the host gene and miR-205 was also noted when comparing the consequences of the miR-205 targeting design on the expression of different *MIR205HG* transcripts (Figure 3A). The distal transcript of *MIR205HG* was not formed in the miR-205 knockout mice, while proximal transcripts were increased 4–5-fold relative to controls (Figures S4A). These findings leave unresolved the role of miR-205 in the anterior pituitary.

To thoroughly ascertain the functional contribution of miR-205 in the anterior pituitary, we developed a different set of miR-205 targeted mice that avoided deleting segments of

the lncRNA (Figures 4C and S6A). A 10-nucleotide substitution was introduced within the seed sequence and stem loop of the miR-205 allele using CRISPR/Cas9 (Figure 4C). Mice harboring seed sequence mutations on both alleles of miR-205 (miR-205$^{KI/KI}$) retained normal transcript levels of *Pit1*, *Zbtb20*, *prolactin*, and *growth hormone* (Figure 4D). These findings firmly establish that *MIR205HG* functions as a lncRNA in controlling endocrine hormone production from the anterior pituitary independent of miR-205. Of note, of the initial 40 founder pups derived from CRISPR/Cas9 genome editing, 10 were runts and 8 were small (Figure S6B–C). DNA sequencing revealed that the runts had internal deletions on both alleles that affected the lncRNA. Those with the correct knock-in mutation of miR-205 were normal in size, further substantiating a principal role of the lncRNA in regulating pituitary functions.

MIR205HG Regulates Prolactin and Growth Hormone Production by Modulating the *Pit1* and *Ztbt20* Transcription Factors

Given that *MIR205HG* regulates growth hormone and prolactin production in the pituitary, we next examined the impact of the targeting of this lncRNA on the pituitary gland itself. The structure and size of the entire pituitary, and the positioning of the anterior pituitary (darker purple) was similar in control and *MIR205HG*-deficient mice (Figure 5A). *In situ* hybridization experiments confirmed expression of *MIR205HG* in the anterior pituitary of control but not knockout mice (Figure 5B). To ascertain whether the number of lactotropes and/or somatotropes were affected by the deletion of *MIR205HG*, immunofluorescence staining was undertaken with anti-prolactin and anti-growth hormone specific antibodies. Cells expressing each hormone were evident in the P14 *MIR205HG*-null animals (Figure 5C). Quantitating the number of cells expressing each hormone revealed no statistically significant differences among the control and *MIR205HG* null animals, indicating that the development of both cell types is not compromised by the targeting of this lncRNA (Figure 5D). This suggests that the overall levels of the hormones produced by these cell types is reduced in the absence of *MIR205HG*.

MIR205HG Regulates *Pit1* and *Zbtb20* in a Rat Lactotrope Cell Line MMQ

MMQ is a rat lactotrope cell line that expresses *Pit1*, *Zbtb20*, *prolactin* and small levels of *growth hormone* (Cao et al., 2016). These cells were analyzed for the presence of a rat homolog of *MIR205HG*. Multiple rat *MIR205HG* transcripts were identified, much like that noted for the murine homolog (Figure 6A). Transcripts for *MIR205HG* were predominantly localized to the nucleus, and less so in the cytoplasm, indicating a putative role for this lncRNA in gene regulation. A distinct lncRNA, *NEAT1*, used as a control, was restricted to the nucleus (Figure 6B). To determine if *MIR205HG* directly affected *Pit1* or *Zbtb20* expression, GapmeRs targeting two different regions in rat *MIR205HG* were transfected into the MMQ cell line and the transcript levels of the lncRNA were assessed (Figure 6C, Table S3). Both GapmeRs, specific for rat *MIR205HG*, reduced expression of transcripts comprising the proximal and central regions of the lncRNA compared to a control GapmeR (Figure 6D). Notably, the knockdown of rat *MIR205HG* diminished expression of rat *Pit1*, *Zbtb20*, *prolactin* and *growth hormone* (Figure 6D). As a complementary approach to the knockdown, lentiviruses over-expressing murine and rat *MIR205HG* were used to infect the MMQ cell line. Elevations in rat *MIR205HG* (*rno-MIR205HG*) and to a lesser extent

murine *MIR205HG* (*mmu-MIR205HG*), increased the levels of rat *Pit1*, *Zbtb20*, *prolactin* and *growth hormone* (Figure 6E). These experiments demonstrate that *MIR205HG* functions as a lncRNA in regulating growth hormone and prolactin in lactotropes.

MIR205HG Enhances the Transcription of Prolactin Gene

To gain mechanistic insights into how *MIR205HG* regulates prolactin, reporter assays were undertaken with the prolactin promoter region of 1.7 kb cloned upstream of luciferase. Consistent with published reports, *Pit1* transcriptionally activates sequences comprising the prolactin promoter (Figure 7A). Neither *MIR205HG* or *Zbtb20* directly activated the prolactin promoter construct (Figure 7A). However, the co-transfection of *MIR205HG* with non-saturating levels of *Pit1* potentiated transcriptional activation of the prolactin promoter (Figure 7A). Co-transfection of *MIR205HG* with *Zbtb20* did not exhibit any transcriptional activity towards the reporter construct, suggesting the effects of the lncRNA are mediated through *Pit1* (Figure 7A). Since *Zbtb20* can increase *Pit1* activity towards the prolactin promoter, we used fixed levels of *Pit1* and *Zbtb20*, and added increasing amounts of *MIR205HG* (Cao et al., 2016). This resulted in a significant enhancement in the transcriptional activation of the prolactin promoter (Figure 7A). The experiments were repeated with a construct comprising the growth hormone promoter. Again, *MIR205HG* was able to potentiate the transcriptional activity of Pit1 towards the growth hormone promoter (Figure 7B).

The *MIR205HG* over-expression assays included an intact pre-mature miR-205 sequence. Since this led to some miR-205 expression in the MMQ cell line, antagomirs that selectively targeted this miRNA were added to the cells (Figure 7C). An antagomir specific for miR-205 completely eliminated the residual levels of this miRNA compared to the control antagomir (Figure 7C). *Pit1*, *Zbtb20*, *prolactin* and *growth hormone* transcript levels were not affected with the selective targeting of miR-205, as their values were similar to control conditions (Figure 7C). These findings support a direct functional role for *MIR205HG* as a lncRNA in promoting *Pit1*/*Zbtb20* transcriptional activities that is independent of miR-205.

The aforementioned experiments suggest that MIR205HG could potentially interact with Pit1. To examine this possibility, HEK293T cells were transfected with a full-length mmu-MIR205HG expression vector in combination with those comprising a FLAG-tagged construct for rat *Pit1* and rat *Zbtb20*. To complement these studies, we also used a full-length construct for MIR205HG wherein the nucleotide substitutions that eliminated the seed sequence and hairpin loop of miR-205 were introduced (mmu-MIR205HG-KI). The transfected cells were subsequently UV-crosslinked, lysed, and control IgG or anti-FLAG immunoprecipitations performed. RNA was isolated from the immunoprecipitations and used in qRT-PCR reactions. Transcripts comprising segments of MIR205HG, detected with primers spanning the lncRNA (Probe 1, Probe 2b, and Probe 2c) were enriched 5–10-fold in the anti-FLAG precipitations relative to control IgG (Figure 7D). Interestingly, these levels were reduced about 2–3-fold when using the KI construct. This suggests that the KI may partially modulate the secondary RNA structure of MIR205HG, resulting in diminished Pit1 interactions (Figure 7D). Importantly, the results support the model that the lncRNA,

MIR205HG, forms an RNA-protein complex with Pit1, either alone or in combination Zbtb20, to promote growth hormone and prolactin production (Figure 7E).

DISCUSSION

MIR205HG is an intergenic long noncoding RNA best known as the host gene for miR-205, an epithelial-specific miRNA. We report herein a functional role for *MIR205HG* as a regulator of endocrine production in the anterior pituitary. Mice lacking *MIR205HG* have a growth delay partly linked to the reduced serum levels of growth hormone and prolactin, hormones produced by the somatotropes and lactotropes of the anterior pituitary, respectively. While the anterior pituitary produces multiple *MIR205HG* transcripts, there are relatively low levels of the embedded miRNA, miR-205. Earlier studies actually reported miR-205 as absent in the pituitary (Bak et al., 2008; Ludwig et al., 2016). While we did notice a reduced level of growth hormone and prolactin in the original miR-205 knockout mice, this was shown to be a consequence of the targeting design, which eliminated a portion of the lncRNA. We developed a distinct set of miR-205 knock-in mice, and these have normal prolactin and growth hormone levels. This result was further substantiated with the use of antagomirs that selectively target miR-205 in the MMQ cell line. *Pit*, *Zbtb20*, *growth hormone*, or *prolactin* transcript levels were normal when all the miR-205 was targeted (Figure 7C). As *MIR205HG* does not have any protein coding potential, the data are consistent with *MIR205HG* functioning as a lncRNA in regulating the anterior pituitary transcriptome (Table S1) (Anderson et al., 2015; Lin et al., 2011).

Mechanistically, *MIR205HG* appears to potentiate the transcriptional activity of *Pit1* towards the *prolactin* and *growth hormone* promoter, both in the absence and presence of *Zbtb20*. We propose a model wherein *MIR205HG* facilitates *Pit1* interactions with the prolactin and growth hormone promoter elements, which is supported by UV-crosslinking studies wherein Pit1 complexes with the MIR205HG RNA (Figure 7). Moreover, as it is known that Pit1 can regulate its own expression, the fact that MIR205HG enhanced the levels of Pit1 further supports a mechanism whereby this protein-lncRNA complex stabilizes Pit1 and/or increases its binding affinity to the Pit1 promoter. Further experiments are addressing the nature of this interaction.

In our analysis of the *MIR205HG*-deficient mice, we found that the reductions in growth hormone and prolactin occur at different developmental stages, revealing a temporal regulation. Reductions in growth hormone are detected prior to prolactin, which occurs several weeks later. This may be linked to *Zbtb20* functions and locus accessibility. *Zbtb20*-null animals suffer from anterior pituitary hypoplasia and growth retardation as a consequence of impaired development of lactotropes, with most animals dying by 4 weeks of age (Cao et al., 2016). The *MIR205HG* knockout mice do not have such damaging phenotypes, likely because *Pit1* and *growth hormone* normalized as the mice aged.

We also noted that the severity of the growth delay in the *MIR205HG* null mice varies somewhat among littermates. Similar variations in growth recovery have been noted in mice lacking the *delta-like ligand 1 homolog* (*dlk1*), which affects the pituitary gland (Cheung et al., 2013; Perez-Castro et al., 2012). The $dlk1^{-/-}$ variations were attributed to differences in

the magnitude of growth hormone deficiency. While we did not notice such variations, it is possible that epigenetic changes may have modulated the severity of the growth delay. This is consistent with our characterization of the initial litters developed from the *MIR205HG* targeting. Fifty percent of the pups were either runts or small sized, and this was likely due to the introduction of indels on both alleles. Some of these pups died, and most did not breed, meaning that we may have selected founders harboring epigenetic modifications that improved endocrine output.

Our findings establish a marked dichotomy in the functions of MIR205HG. In the anterior pituitary, it predominates as a lncRNA. In epithelial cells of the skin and thymus, it primarily serves as the host gene for miR-205. The small levels of miR-205 produced in the anterior pituitary relative to the skin and thymus may be explained by the selective expression of two transcription factors, ΔNp63 or Foxn1 in the epithelial cells of the latter two tissues. Neither transcription factor is expressed in the anterior pituitary (Blackburn et al., 1996; Bredenkamp et al., 2014; Di Como et al., 2002; Hoover et al., 2016; Su et al., 2015). ΔNp63 binds at a site 1 kb upstream of miR-205, and enhances the expression of the miRNA (Figure S2F) (Tran et al., 2013). In the thymus, miR-205 is restricted to thymic epithelial cells, which develop via the master transcriptional regulator Foxn1 (Vaidya et al., 2016). CHIP-Seq data of Foxn1 immunoprecipitations revealed a binding site upstream of pre-miR-205 (Figure S2F) (Žuklys et al., 2016). The dual functions of MIR205HG as a lncRNA and the host gene for miR-205 is also supported by our gene expression data. Comparing the transcriptomes of the pituitary and skin in normal, *MIR205HG*$^{-/-}$, and miR-205$^{-/-}$ female mice indicates that the *MIR205HG*-deficiency causes a unique up- and down- regulation of many mRNAs in the pituitary tissue as opposed to the skin (Figure S7B–D). We suggest the small number of genes coordinately up- and down- regulated in the pituitary when comparing both *MIR205HG* and miR-205 null animals is a consequence of the deletion of a segment of the lncRNA due to the targeting of miR-205. Contrasting the distinct transcript regulation in the pituitary between these noncoding RNAs, a remarkable overlap in the mRNAs regulated by MIR205HG versus miR-205 was apparent in the skin (Figure S7B and D). We further compared the functions of *MIR205HG* relative to miR-205 in the thymus as miR-205 mitigates the stress-induced hypoplasia that occurs in this tissue (Figure S4C–D) (Belkaya et al., 2011; Hoover et al., 2016). We generated conditional knockout lines for *MIR205HG* using the *Foxn1*-cre transgenic line, which provides for a selective expression of Cre recombinase in thymic epithelial cells (Gordon et al., 2007). The mice were injected with polyinosinic:polycytidylic acid (polyI:C) to elicit a transient stress-mediated thymic hypoplasia due to interferon elevations (Hoover et al., 2016). The thymus weight, overall cellularity, and numbers of different thymocyte subsets was less in the *MIR205HG*$^{fl/fl}$:*Foxn1*-Cre lines compare to littermate treated controls that matched the more severe hypoplasia we had reported previously with the miR-205$^{fl/fl}$:*Foxn1*-Cre mice (data not shown) (Hoover et al., 2016). The stress-regulated functions of miR-205 may explain the post-natal lethality and hair follicle regeneration defects originally reported for the knockout mice (Farmer et al., 2017; Farmer et al., 2013; Park et al., 2012; Wang et al., 2013). These phenotypes were not readily replicated in the same set of miR-205 conditional knockout mice bred in our facility. This again reveals a variable penetrance, with the loss of

miR-205 resulting in more tissue damage and/or less recovery following stress, elicited by infections, environmental changes, and/or microbiome fluctuations.

In summary, *MIR205HG* functions as a lncRNA in the anterior pituitary gland, initially detected in Rathke's pouch from wherein the pituitary is specified during embryogenesis. We propose that *MIR205HG* modulates the transcriptional activity and/or accessibility of *Pit1* and *Zbtb20* towards *Pit1*, *growth hormone*, and *prolactin* promoters in multiple species.

STAR METHODS

Detailed methods are provided in the online version of this paper and include the following:

CONTACT FOR REAGENT AND RESOURCE SHARING

Further information and requests for resources and reagents should be directed to and will be fulfilled by the Lead Contact, Nicolai S.C. van Oers (Nicolai.vanoers@utsouthwestern.edu).

EXPERIMENTAL MODEL AND SUBJECT DETAIL

Mice—Animal work described in this manuscript has been approved and conducted under the oversight of the UT Southwestern Institutional Animal Care and Use Committee (APN numbers 2010-0053 and 2015-101247). Mice were housed in both specific pathogen-free facility and conventional rooms at UT Southwestern Medical Center. The *MIR205HG* targeted mice and miR-205 knock in mice were developed entirely on a C57BL/6 background (see subsequent section). The *MIR205TM* conditional knockout mice (miR-205 KO) were generated by the International Knockout Mouse Consortium and acquired from the Jackson Lab (MGI:2676880) (Park et al., 2012). As described elsewhere, these were backcrossed onto C57BL/6 mice for 11 generations (Hoover et al., 2016). The FlpO-recombinase mice were acquired from the Mutant Mouse Regional Resource Centers (C57BL/6, MGI:4415609) (Birling et al., 2012). The *Foxn1*-Cre line was obtained from The Jackson Laboratory (on a C57BL/6 background). The experiments were designed with male and female mice as separate experimental cohorts. This included those used for gene expression comparisons, serum measurements for prolactin and growth hormone, and measurements of different transcripts. These are indicated in the text and/or figure legends. For experiments pertaining to embryos, the sex was not determined.

METHOD DETAILS

Cell Lines—Human embryonic kidney cells HEK293T (ATCC CRL-3216) and a rat lactotrope cell line MMQ (ATCC CRL-10609) were obtained from American Type Culture Collection (ATCC, Manassas, VA). HEK293T cells were grown in standard DMEM-media containing 10% FBS with penicillin, streptomycin and HEPES. The pituitary cell line was grown in F-12K medium containing 2.5% FBS and 15% horse serum along with antibiotics.

Conditional targeting of the murine MIR205HG and generation of the miR-205 knock in line—Genomic DNA, prepared from C57BL/6 male mice, was used to subclone the left and right arms of MIR205HG into the targeting construct, pGKneoF2L2dta (Addgene plasmid #13445). The orientation of murine MIR205HG and miR-205 extended

from left to right, as designated in the ncbi genome browser. The 2.3 kb right arm contained the 5' regulatory elements of the lncRNA (MIR205.001). Xba I and Hind III restriction sites were engineered at the ends of the genomic DNA to enable subcloning into the targeting vector. The left arm contained exons 1 and 2, with miR-205 encoded within the distal 3' end of exon 2. A 4-part cloning strategy was required for this. First, a 1 kb fragment containing a pre-existing Bam HI restriction site within the genomic DNA was subcloned into the pCR2.1 TOPO-TA cloning vector (Stratagene, Inc., La Jolla, CA). A second 1.46 kb genomic fragment was cloned using existing Bam HI site along with an engineered Bam HI site, which extended the length of the genomic fragment to 2.46 kb. The Bam HI site introduced for cloning was subsequently removed by site-directed mutagenesis. The plasmid containing the genomic fragment with the remaining Bam HI site was cut, treated with alkaline phosphatase, and a loxP site was introduced at this position using overlapping oligonucleotides containing the entire loxP site (Oligo 933; Oligo 934). Site directed mutagenesis eliminated an overlapping Xba I/Eco RV site within MIR205HG. A 400 bp piece was appended to the 2.566 fragment with the introduction of a Pvu I restriction site. This was necessitated because of a 60 nucleotide AT rich segment within the genome could not be amplified by PCR. Overlapping oligonucleotides containing this AT-rich segment (985/986) were ligated into the Pvu I site. An additional 2 kb genomic piece was cloned into the left arm, resulting in the generation of 4.1 kb fragment. The right arm was subsequently cloned into the Hind III/Nhe I site of pgkneoF2L2dta, after the targeting vector was cut with Hind III and Xba I. The left arm was cloned into the Not I/Xma I site present in pgkneoF2L2dta. The conditional allele was given the name pGKF22LdtalncKI#3. A linearized vector was purified and provided to the Transgenic Core at UT Southwestern Medical Center. The construct was electroporated into C57BL/6N-derived ES cells (JM8) that were obtained from the Knockout Mouse Project Repository (KOMP). Southern blotting was used to identify ES cells with the targeted allele following Eco RV digests. Of three clones obtained, one ES cell clone, 4H11, was selected for further propagation. This line was injected into albino B6 blastocysts, and 7 distinct chimeric male mice were recovered. The percent chimerism ranged from 20–90%. The miR-205 knock-in line was developed using CRISPR/Cas9 technologies offered by the Transgenic and Knockout core at UT Southwestern Medical Center. The guide RNA was developed to target the ngg site within miR-205. A single stranded oligonucleotide containing the repair template was synthesized by Idt technologies and used for the homologous recombination.

RNA isolation and analysis—RNA was isolated using the miRNAeasy kit (Qiagen Inc., Germantown, MD) or the miRVANA kit (Ambion, Thermo-Fisher) for skin, pituitary, and hypothalamus tissue samples. Contaminating DNA was removed by DNAse I digestion (Ambion, Thermo-Fisher) and the remaining RNA was purified with an RNA clean up step (RNA-5, Zymo Research Inc.). cDNA was generated with 1 μg of RNA using the High Capacity cDNA reverse transcription kit (Applied Biosystems Inc., Foster City, CA). Oligo-dT priming was used for reverse transcription as it was much more effective at generating *MIR205HG* transcripts than random prime methods. RT-PCR was performed with 100 ng of cDNA using LA Taq Polymerase (Clontech Inc., Mountain View, CA). The PCR conditions were as follows: 98°C for 10 seconds, 59°C for 30 seconds, 72°C for 2 minutes, repeated 34x, followed by 72°C for 5 minutes, yielding a 1.6 kb PCR product.

Primers used for PCR reactions are listed (Supplemental Table 2). Northern blot analysis for miRNAs was performed as previously described (Belkaya et al., 2011). Gene expression was performed as described (Khan et al., 2016). For gene expression comparisons, the Affymetrix Clariom S™ mouse array was used, which focuses on 20,000 well annotated genes (Thermo-Fisher Scientific). Transcriptomic analysis was done using TruSeq Stranded Total RNA kit (Catalog# RS-122-2301) from Illumina. RNA sequencing (RNAseq) libraries were validated on an Agilent Bioanalyzer 2100. RNAseq libraries were sequenced on a SE50 (single end 50 base pair) Hiseq 2500 lane, which yielded an average of about 25 Million reads/sample. We used CLC Bio Genomics Workbench 7 and Golden Helix genome browser for bioinformatics analysis of the sequencing data. This approach is used by CLC Genomics Workbench. Mouse genome (MM10) was used as reference to map the raw sequencing reads. All uniquely mapped and unmapped reads were counted. Alignment with mismatch cost of “2”, Insertion cost”3” Deletion cost of “3” was used. The maximum number of hits for a read was set to 1 meaning that only reads those maps uniquely were considered. The steady state expression of various genes was calculated in terms of RPKM values and BAM files were generated for coverage visualization (Mortazavi et al., 2008).

UV-crosslinking, protein isolation and qRT-PCR assays—Ten cm dishes containing 70% confluent HEK293 T cells were used in transfection assays to assay for protein-RNA interactions. The assays were carried out as described in detail with the following modifications (Sei and Conrad, 2014). For the lysis, RIPA correction, and RIPA buffers, cRNA was excluded. Forty-eight hrs post-transfection, the cells were UV-crosslinked at 150 mJ/cm^2. The cells were harvested in calcium/magnesium free PBS and flash frozen in liquid N_2. The pellet was thawed, processed for 5 min at 65°C in 140 µl SDS-buffer. After cooling on ice, 560 µl of RIPA correction buffer was added, the cells pipetted several times, and the material sheared in a Qiagen DNA shredder twice. The samples in the flow-through were processed for immunoprecipitations using 3 µg of control IgG or anti-FLAG-IgG pre-bound to 30 µl of protein A/G containing magnetic beads (Sigma). Following a 2–3 hr immunoprecipitation at 4°C, the precipitates were washed 4X in RIPA buffer. Residual protein was digested in the presence of Proteinase K for 3 hrs, remaining RNA material was precipitated in ETOH and digested with DNAase. The samples were applied to an RNA Quick and Clean column (Zymo Research) prior to use in qRT-PCR assays.

Real time PCR and primers sequence—cDNAs were generated using High Capacity cDNA reverse transcription kit with random primers. MicroRNA cDNAs were synthesized using miRCURY LNA™ RT kit (Qiagen). Real time PCR was performed with Maxima SYBR Green master mix (Thermo Fisher Scientific) on QuantStudio 7 equipment. The primer sequences used for real time PCR are listed in Supplementary Table 1. Relative expression levels of genes were calculated by normalizing to control genes (PPIA, GAPDH), and the expression of microRNAs were normalized to 5sRNA. Data is presented as fold change compared to control conditions.

Tissue processing and staining—Embryos obtained from timed pregnant mice (e8.5–18.5) and pituitary gland from adult mice were fixed in 4% paraformaldehyde (PFA) at 4°C overnight. The processing of these tissues and *in situ* staining experiments were performed

as described elsewhere (Azizoglu et al., 2016). Hematoxylin and Eosin (H&E) staining of pituitary gland was performed using standard protocol and imaged on an Aziovert 200M inverted fluorescent microscope. For immunofluorescence staining, sections were incubated with primary antibodies (1:100, rabbit anti-prolactin (PRL), and rabbit anti-growth hormone (GH) from the National Hormone & Peptide Program, NHPP) at 4°C overnight. The next day, sections were washed with PBS and stained with Alexa Fluo 488 conjugated goat anti-rabbit secondary antibody (1:200, Invitrogen). Tissues were then stained with DAPI and mounted with ProLong™ Gold antifade mountant with DAPI (Thermo Fisher Scientific). Images were taken on a Leica confocal microscope.

Riboprobe synthesis—RNA isolated from whole thymus was used to amply a 1.3 kb piece of MIR205HG and cloned into the pBluescript vector (Stratagene). The template was linearized with Hind III (Thermo-Fisher, Inc.) and a Digoxigenin (Dig) UTP antisense riboprobe was synthesized by the addition of T7 RNA polymerase (Roche). *Gcm2*, *Foxn1*, and *Pitx2* riboprobes were generated in a similar manner using primers previously described (Supplemental Table 2) (Farmer et al., 2013; Hoover et al., 2016; Potter et al., 2011; Xu et al., 2009).

Modulation of MIR205HG and miR-205 in MMQ Cells—MMQ cells (2.5×10^6 cells) were re-suspended in 100 μl PBS and mixed with LNA™ GapmeR controls or sequences designed to target different locations in the rat MIR205HG homolog (2.5 μM final concentration) (Supplemental Table 3) (Qiagen Corp.). The LNA™ GapmeRs were delivered into MMQ cells using an Amaxa Nucleofactor. 24 and 48 hrs post transfection, the cells were harvested for RNA isolation. The miRCURY LNA™ miR-205 inhibitors and controls were purchased from Qiagen (Supplemental Table 2). 500 nM inhibitors or controls were added directly into MMQ cells for 48 hrs before harvested.

Overexpression of mouse and rat MIR205HG in MMQ cells using lentiviral infection—Mouse and rat *MIR205HG* sequences were cloned into pCDH-CMV lentiviral vector. Recombinant plasmids together with packaging vectors were transfected into HEK293T cells for producing lentivirus. Lentivirus was harvested from supernatants and used to infect MMQ cells for 72 hrs. Puromycin (3 μg/ml) was added to select the stable cells expressing mouse and rat MIR205HG. Six days later, MMQ cells were processed for RNA isolation.

QUANTIFICATION AND STATISTICAL ANALYSIS

Statistical significance was determined by Student’s t test comparing the wildtype control with various samples. P-value < 0.05 was considered statistically significant. The p values provided are determined using GraphPrism.

Supplementary Material

Refer to Web version on PubMed Central for supplementary material.

ACKNOWLEDGEMENTS

We would like to thank Angela Mobley and Ian Mathews from the flow cytometry core for assistance in TEC sorting and flow analyses. We appreciate the input from Ms. Fatma Coskun (van Oers laboratory) in RNA-protein studies. We are grateful for the help provided by Drs. Leilani Marty-Santos and Caitlyn Braisch in Dr. Ondine Cleaver's laboratory. We are very thankful for help with RNA-protein interaction studies from Ms. Anu Thomas (Mendell laboratory), and Dr. Nicholas Conrad and Mr. Ian Boys (Department of Microbiology, UT Southwestern Medical Center). We thank Drs. Rhonda Bassel-Duby and Eric Olson for helpful discussions, and Mr. Jose Cabrera for image preparations (Department of Molecular Biology at UT Southwestern Medical Center). Dr. James Richardson, John Shelton and staff provided help with the processing of pituitary tissue and lacrimal glands and are part of the histology core. The *MIR205HG* targeted mice and miR-205 knock-in mice were generated with the help of Dr. Robert Hammer and staff from the Transgenic and Knockout Core at UT Southwestern Medical Center. The primary antibodies used to identify pituitary cell lineages were provided by Dr. A. F. Parlow from the Harbor-UCLA Research and Education Institute. The ΔNp63 construct was graciously sent by Dr. S. Sinha (University at Buffalo, NY). This work was supported, in part, by grants from the National Institutes of Health R01 (AI114523, NvO), F31 (AI110140, AH); as well as Children's Medical Center Research Bridge Support (NvO and MdlM), Beecherl funds from the Department of Immunology at UT Southwestern Medical Center (NvO), and the Jeffrey Modell Foundation (MdlM).

REFERENCES

Andersen B, and Rosenfeld MG (2001). POU Domain Factors in the Neuroendocrine System: Lessons from Developmental Biology Provide Insights into Human Disease*. Endocrine Reviews 22, 2–35. [PubMed: 11159814]

Anderson DM, Anderson KM, Chang CL, Makarewich CA, Nelson BR, McAnally JR, Kasaragod P, Shelton JM, Liou J, Bassel-Duby R, et al. (2015). A micropeptide encoded by a putative long noncoding RNA regulates muscle performance. Cell 160, 595–606. [PubMed: 25640239]

Angrand PO, Vennin C, Le Bourhis X, and Adriaenssens E (2015). The role of long non-coding RNAs in genome formatting and expression. Front Genet 6, 165. [PubMed: 25972893]

Azizoglu DB, Chong DC, Villasenor A, Magenheim J, Barry DM, Lee S, Marty-Santos L, Fu S, Dor Y, and Cleaver O (2016). Vascular development in the vertebrate pancreas. Dev Biol 420, 67–78. [PubMed: 27789228]

Bak M, Silahtaroglu A, Møller M, Christensen M, Rath MF, Skryabin B, Tommerup N, and Kauppinen S (2008). MicroRNA expression in the adult mouse central nervous system. RNA 14, 432–444. [PubMed: 18230762]

Belkaya S, Silge RL, Hoover AR, Medeiros JJ, Eitson JL, Becker AM, de la Morena MT, Bassel-Duby RS, and van Oers NS (2011). Dynamic modulation of thymic microRNAs in response to stress. PLoS ONE 6, e27580. [PubMed: 22110677]

Birling M-C, Dierich A, Jacquot S, Hérault Y, and Pavlovic G (2012). Highly-efficient, fluorescent, locus directed cre and FlpO deleter mice on a pure C57BL/6N genetic background. genesis 50, 482–489. [PubMed: 22121025]

Blackburn CC, Augustine CL, Li R, Harvey RP, Malin MA, Boyd RL, Miller JF, and Morahan G (1996). The nu gene acts cell-autonomously and is required for differentiation of thymic epithelial progenitors. Proceedings of the National Academy of Sciences of the United States of America 93, 5742–5746. [PubMed: 8650163]

Bredenkamp N, Nowell CS, and Blackburn CC (2014). Regeneration of the aged thymus by a single transcription factor. Development (Cambridge, England) 141, 1627–1637.

Cao D, Ma X, Cai J, Luan J, Liu A-J, Yang R, Cao Y, Zhu X, Zhang H, Chen Y-X, et al. (2016). ZBTB20 is required for anterior pituitary development and lactotrope specification. Nature Communications 7, 11121.

Cesana M, Cacchiarelli D, Legnini I, Santini T, Sthandier O, Chinappi M, Tramontano A, and Bozzoni I (2011). A long noncoding RNA controls muscle differentiation by functioning as a competing endogenous RNA. Cell 147, 358–369. [PubMed: 22000014]

Chang T-C, Pertea M, Lee S, Salzberg SL, and Mendell JT (2015). Genome-wide annotation of microRNA primary transcript structures reveals novel regulatory mechanisms. Genome Research 25, 1401–1409. [PubMed: 26290535]

Cheung LYM, Rizzoti K, Lovell-Badge R, and Tissier PR (2013). Pituitary Phenotypes of Mice Lacking the Notch Signalling Ligand Delta-Like 1 Homologue. Journal of Neuroendocrinology 25, 391–401. [PubMed: 23279263]

De Cola A, Volpe S, Budani MC, Ferracin M, Lattanzio R, Turdo A, D'Agostino D, Capone E, Stassi G, Todaro M, et al. (2015). miR-205–5p-mediated downregulation of ErbB/HER receptors in breast cancer stem cells results in targeted therapy resistance. Cell Death Dis 6, e1823. [PubMed: 26181203]

Dey BK, Pfeifer K, and Dutta A (2014). The H19 long noncoding RNA gives rise to microRNAs miR-675–3p and miR-675–5p to promote skeletal muscle differentiation and regeneration. Genes Dev 28, 491–501. [PubMed: 24532688]

Di Como CJ, Urist MJ, Babayan I, Drobnjak M, Hedvat CV, Teruya-Feldstein J, Pohar K, Hoos A, and Cordon-Cardo C (2002). p63 expression profiles in human normal and tumor tissues. Clin Cancer Res 8, 494–501. [PubMed: 11839669]

Farmer DJT, Finley JK, Chen FY, Tarifeño-Saldivia E, McNamara NA, Knox SM, and McManus MT (2017). miR-205 is a critical regulator of lacrimal gland development. Developmental Biology 427, 12–20. [PubMed: 28511845]

Farmer DT, Shariat N, Park CY, Liu HJ, Mavropoulos A, and McManus MT (2013). Partially penetrant postnatal lethality of an epithelial specific MicroRNA in a mouse knockout. PLoS One 8, e76634. [PubMed: 24116130]

Gong S, Miao Y-L, Jiao G-Z, Sun M-J, Li H, Lin J, Luo M-J, and Tan J-H (2015). Dynamics and Correlation of Serum Cortisol and Corticosterone under Different Physiological or Stressful Conditions in Mice. PLOS ONE 10.

Gordon J, Xiao S, Hughes B, Su D. m., Navarre S, Condie B, and Manley N (2007). Specific expression of lacZ and cre recombinase in fetal thymic epithelial cells by multiplex gene targeting at the Foxn1 locus. BMC developmental biology 7, 69. [PubMed: 17577402]

Gregory PA, Bert AG, Paterson EL, Barry SC, Tsykin A, Farshid G, Vadas MA, Khew-Goodall Y, and Goodall GJ (2008). The miR-200 family and miR-205 regulate epithelial to mesenchymal transition by targeting ZEB1 and SIP1. Nat Cell Biol 10, 593–601. [PubMed: 18376396]

Hoover AR, Dozmorov I, MacLeod J, Du Q, de la Morena MT, Forbess J, Guleserian K, Cleaver OB, and van Oers NS (2016). MicroRNA-205 Maintains T Cell Development following Stress by Regulating Forkhead Box N1 and Selected Chemokines. J Biol Chem 291, 23237–23247. [PubMed: 27646003]

Horseman ND, Zhao W, Montecino-Rodriguez E, Tanaka M, Nakashima K, Engle SJ, Smith F, Markoff E, and Dorshkind K (1997). Defective mammopoiesis, but normal hematopoiesis, in mice with a targeted disruption of the prolactin gene. The EMBO Journal 16, 6926–6935. [PubMed: 9384572]

Kelberman D, Rizzoti K, Lovell-Badge R, Robinson ICAF, and Dattani MT (2009). Genetic Regulation of Pituitary Gland Development in Human and Mouse. Endocrine Reviews 30, 790–829. [PubMed: 19837867]

Keniry A, Oxley D, Monnier P, Kyba M, Dandolo L, Smits G, and Reik W (2012). The H19 lincRNA is a developmental reservoir of miR-675 that suppresses growth and Igf1r. Nat Cell Biol 14, 659–665. [PubMed: 22684254]

Khan S, Kuruvilla M, Hagin D, Wakeland B, Liang C, Vishwanathan K, Gatti RA, Torgersen TR, Abraham RS, Wakeland EK, et al. (2016). RNA sequencing reveals the consequences of a novel insertion in dedicator of cytokinesis-8. J Allergy Clin Immunol 138, 289–292 e286. [PubMed: 26883462]

Kopp F, and Mendell JT (2018). Functional Classification and Experimental Dissection of Long Noncoding RNAs. Cell 172, 393–407. [PubMed: 29373828]

LaPensee CR, Horseman ND, Tso P, Brandebourg TD, Hugo ER, and Ben-Jonathan N (2006). The Prolactin-Deficient Mouse Has an Unaltered Metabolic Phenotype. Endocrinology 147, 4638–4645. [PubMed: 16809445]

Lee S, Kopp F, Chang T-C, Sataluri A, Chen B, Sivakumar S, Yu H, Xie Y, and Mendell Joshua T. (2016). Noncoding RNA NORAD Regulates Genomic Stability by Sequestering PUMILIO Proteins. Cell 164, 69–80. [PubMed: 26724866]

Lin MF, Jungreis I, and Kellis M (2011). PhyloCSF: a comparative genomics method to distinguish protein coding and non-coding regions. Bioinformatics 27, i275–282. [PubMed: 21685081]

Ludwig N, Leidinger P, Becker K, Backes C, Fehlmann T, Pallasch C, Rheinheimer S, Meder B, Stähler C, Meese E, et al. (2016). Distribution of miRNA expression across human tissues. Nucleic Acids Research 44, 3865–3877. [PubMed: 26921406]

Mortazavi A, Williams BA, McCue K, Schaeffer L, and Wold B (2008). Mapping and quantifying mammalian transcriptomes by RNA-Seq. Nat Meth 5, 621–628.

Park C, Jeker L, Carver-Moore K, Oh A, Liu H, Cameron R, Richards H, Li Z, Adler D, Yoshinaga Y, et al. (2012). A resource for the conditional ablation of microRNAs in the mouse. Cell reports 1, 385–391. [PubMed: 22570807]

Perez-Castro C, Renner U, Haedo MR, Stalla GK, and Arzt E (2012). Cellular and Molecular Specificity of Pituitary Gland Physiology. Physiological Reviews 92, 1–38. [PubMed: 22298650]

Potter CS, Pruett ND, Kern MJ, Baybo MA, Godwin AR, Potter KA, Peterson RL, Sundberg JP, and Awgulewitsch A (2011). The nude mutant gene Foxn1 is a HOXC13 regulatory target during hair follicle and nail differentiation. J Invest Dermatol 131, 828–837. [PubMed: 21191399]

Qin A-Y, Zhang X-W, Liu L, Yu J-P, Li H, Emily Wang S-Z, Ren X-B, and Cao S (2013). MiR-205 in cancer: An angel or a devil? European Journal of Cell Biology 92, 54–60. [PubMed: 23279926]

Quinn JJ, and Chang HY (2016). Unique features of long non-coding RNA biogenesis and function. Nat Rev Genet 17, 47–62. [PubMed: 26666209]

Sakai K, and Miyazaki J (1997). A transgenic mouse line that retains Cre recombinase activity in mature oocytes irrespective of the cre transgene transmission. Biochem Biophys Res Commun 237, 318–324. [PubMed: 9268708]

Sei E, and Conrad NK (2014). UV cross-linking of interacting RNA and protein in cultured cells. Methods Enzymol 539, 53–66. [PubMed: 24581438]

Su M, Hu R, Jin J, Yan Y, Song Y, Sullivan R, and Lai L (2015). Efficient in vitro generation of functional thymic epithelial progenitors from human embryonic stem cells. Scientific Reports 5, 9882. [PubMed: 26044259]

Tran MN, Choi W, Wszolek MF, Navai N, Lee ILCL, Nitti G, Wen S, Flores ER, Siefker-Radtke A, Czerniak B, et al. (2013). The p63 Protein Isoform ΔNp63α Inhibits Epithelial-Mesenchymal Transition in Human Bladder Cancer Cells: ROLE OF MIR-205. The Journal of biological chemistry 288, 3275–3288. [PubMed: 23239884]

Tucci P, Agostini M, Grespi F, Markert EK, Terrinoni A, Vousden KH, Muller PAJ, Dötsch V, Kehrloesser S, Sayan BS, et al. (2012). Loss of p63 and its microRNA-205 target results in enhanced cell migration and metastasis in prostate cancer. Proceedings of the National Academy of Sciences 109, 15312–15317.

Ulitsky I, Shkumatava A, Jan CH, Sive H, and Bartel DP (2011). Conserved function of lincRNAs in vertebrate embryonic development despite rapid sequence evolution. Cell 147, 1537–1550. [PubMed: 22196729]

Vaidya HJ, Briones Leon A, and Blackburn CC (2016). FOXN1 in thymus organogenesis and development. European Journal of Immunology 46, 1826–1837. [PubMed: 27378598]

Wang D, Zhang Z, O'Loughlin E, Wang L, Fan X, Lai E, and Yi R (2013). MicroRNA-205 controls neonatal expansion of skin stem cells by modulating the PI(3)K pathway. Nature cell biology 15, 1153–1163. [PubMed: 23974039]

Xu K, Chong DC, Rankin SA, Zorn AM, and Cleaver O (2009). Rasip1 is required for endothelial cell motility, angiogenesis and vessel formation. Dev Biol 329, 269–279. [PubMed: 19272373]

Yang L, Froberg JE, and Lee JT (2014). Long noncoding RNAs: fresh perspectives into the RNA world. Trends Biochem Sci 39, 35–43. [PubMed: 24290031]

Zhou J, Yang L, Zhong T, Mueller M, Men Y, Zhang N, Xie J, Giang K, Chung H, Sun X, et al. (2015). H19 lncRNA alters DNA methylation genome wide by regulating S-adenosylhomocysteine hydrolase. Nat Commun 6, 10221. [PubMed: 26687445]

Zhu X, Gleiberman AS, and Rosenfeld MG (2007). Molecular physiology of pituitary development: signaling and transcriptional networks. Physiol Rev 87, 933–963. [PubMed: 17615393]

Žuklys S, Handel A, Zhanybekova S, Govani F, Keller M, Maio S, Mayer CE, Teh H, Hafen K, Gallone G, et al. (2016). Foxn1 regulates key target genes essential for T cell development in postnatal thymic epithelial cells. Nature immunology 17, 1206–1215. [PubMed: 27548434]

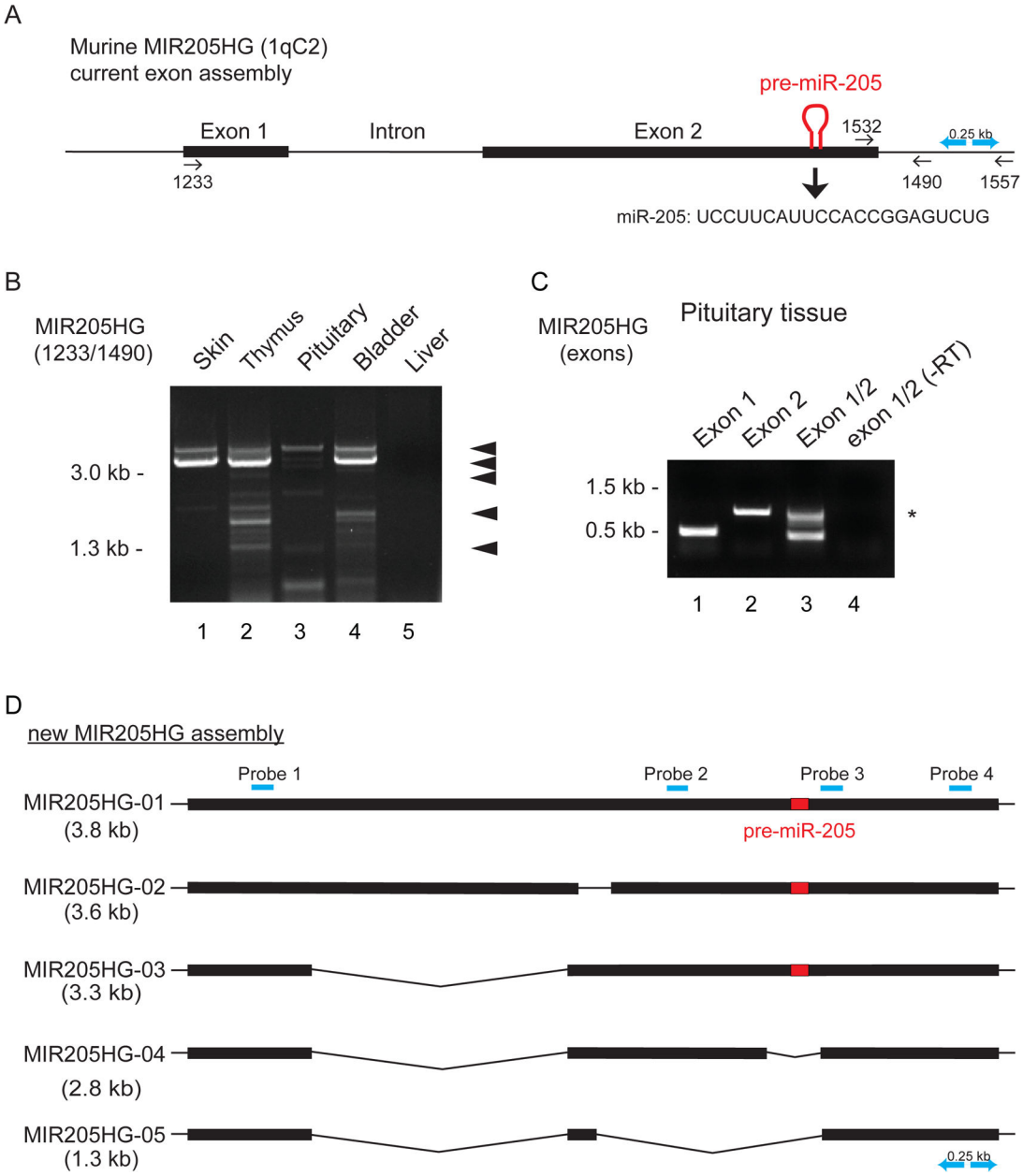

Figure 1.

Tissues comprising epithelial cells express multiple transcripts encoding the lncRNA, MIR205HG, the host gene for miR-205. A. Schematic of the current transcript annotation of mmu-miR-205 and the surrounding lncRNA, *MIR205HG*, which comprises 2 exons. The red segment is the location of mmu-miR-205. B. RT-PCR was performed on RNA derived from the skin, thymus, pituitary, bladder, and liver prepared from 5–6-week-old female mice. Primers for reactions (1233/1490 and 1233/1557) are indicated in Figure 1A. Multiple transcripts, ranging in size from 0.7 kb to 3.8 kb, were identified. C. Primers specific for exon 1 (1233/1234), exon 2 (863/864), and a pair comprising the distal end of exon1 and proximal region of exon 2 (1478/1479) were used in RT-PCR reactions with RNA prepared from the pituitary tissue (Fig. 1A). The asterisk indicates a transcript that reads through the

intronic region, verified by sequencing. No bands were detected in the absence of reverse transcriptase (-RT). D. A transcriptome map of *MIR205HG* was developed following the sequencing of the various transcripts cloned from the gels in Figure 1B and C. The presence of these transcripts for the different tissues, skin (S), thymus (T), pituitary (P), bladder (B) is shown. The sequencing reactions were confirmed with 2–6 independent clones using 4–6 separate tissue isolations with age-matched 5–6-week-old female mice.

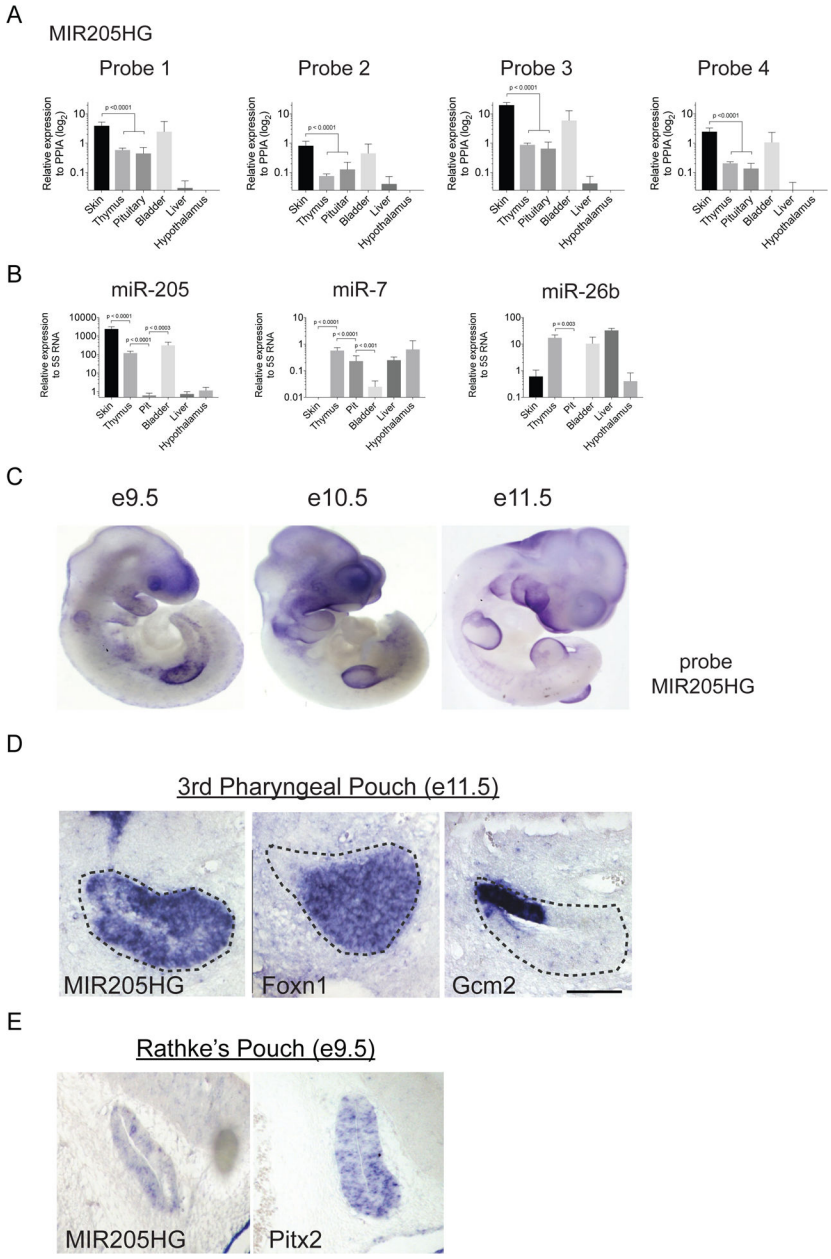

Figure 2.

MIR205HG and miR-205 are differentially expressed in the anterior pituitary, with the lncRNA transcribed as early as e9.5 in embryos. A. Quantitative RT-PCR was used to compare the transcript levels of exon 1 (Probe 1, primers 1403/1406), the proximal region of exon 2 (Probe 2, primers 945/946), distal to miR-205 (Probe 3, primers 1490/1532), and at the 3'-end of the lncRNA (Probe 4, primers 1621/1622). RNA was prepared from the skin, thymus, pituitary, bladder, liver, and hypothalamus (4 female mice, 6-weeks of age). The relative expression was calculated by $\Delta\Delta C_T$, normalized to the endogenous peptidylpropyl isomerase A (*PPIA*) levels. The results were confirmed in 3 independent experiments, with reactions performed in quadruplicate. B. MiR-205, miR-7, and miR-26b expression was assessed by quantitative microRNA RT-PCR using primers specific for each miRNA. The

small RNAs were normalized with a 5S specific probe. P values are shown for the data using 4 mice per group, with data determined mean +/− SEM (students t-test and/or two-way ANOVA). C-E. *In situ* hybridization reveals a spatiotemporal expression of the *MIR205HG* in selected regions of the developing embryo. C. Embryos isolated from the indicated time points were probed with an antisense RNA specific for murine *MIR205HG*, revealing expression in the pharyngeal pouches, limb buds, and telencephalon. In the middle image, the tip of the tail was lost during processing. D. The 3rd pharyngeal pouches from e11.5 embryos were processed and probed for *MIR205HG*, *Foxn1*, and *Gcm2*. E. The brain region encompassing Rathke's pouch, which forms the anterior pituitary tissue, was isolated from e9.5 embryos and probed with *MIR205HG* and *Pitx2* (pituitary) antisense RNAs. Images in C-E are representative of 3 or more independently processed tissues.

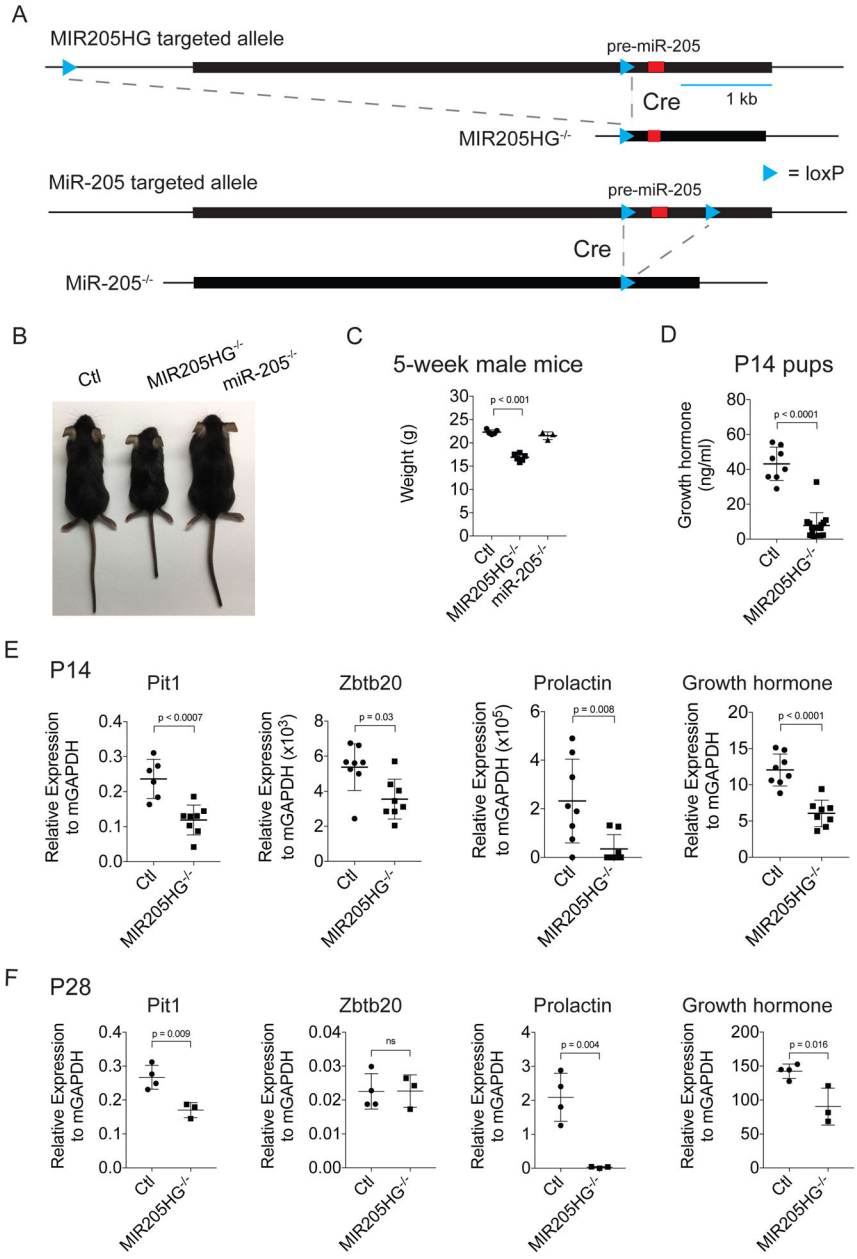

Figure 3.

Growth delay and reduced growth hormone production in mice with a targeted deletion of *MIR205HG*. A. Schematic of the targeting design for *MIR205HG*, which incorporated loxP sites upstream of the first exon and 5' to the pre-mature miR-205 sequence. Conditional and complete knockout mice were generated by breeding the mice with *CAG*-Cre, *Foxg1*-Cre, and *Foxn1*-Cre lines. LoxP sites are denoted in blue and the pre-mature miR-205 with a red box. The previously developed miR-205 knockout line, where loxP sites were placed 5' and 3' to the pre-mature miR-205 sequence is also shown. B. The overall appearance of age-matched 4-week old littermate controls, *MIR205HG*-deficient and a separate mouse lacking miR-205 is shown. The distal segment of the tail was cut for typing purposes. C. The weights of 5-week-old C57BL/6 control mice were compared with *MIR205HG* and

miR-205 knockout lines. The mice were housed in side-by-side cages and female mice were used. D. Growth hormone levels were measured by ELISA using serum samples from the indicated P14 mice. E-F. RNA was isolated from the pituitary using P14 (E) and P28 (F) pups and used for qRT-PCR reactions with primers specific for *Pit1*, *Zbtb20*, *prolactin*, and *growth hormone*. Data represent an analysis using a minimum of 6 animals/group. P values are indicated for those with significant differences (students t-test and two-way ANOVA). ns indicates no significant difference.

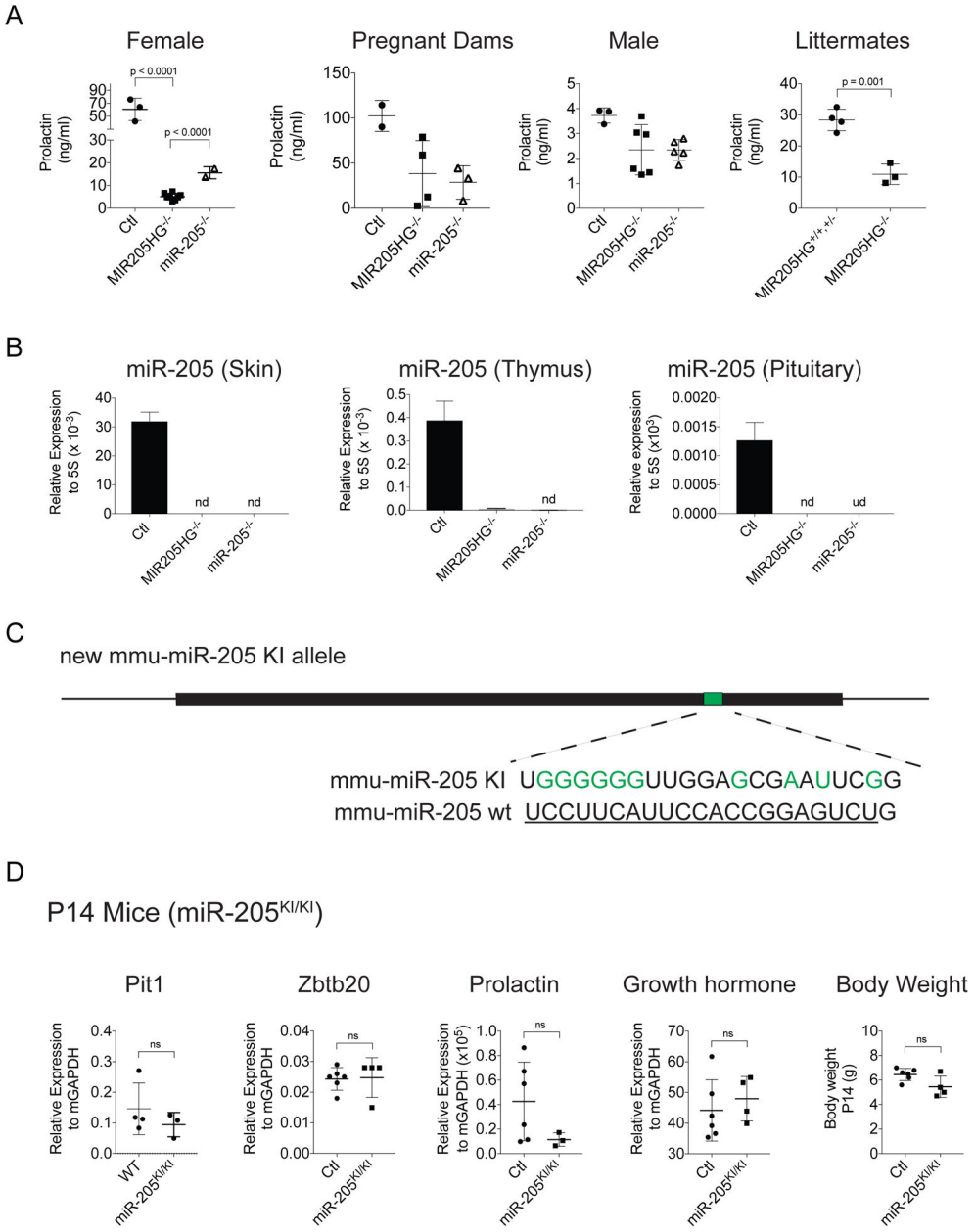

Figure 4.

Endocrine hormones are selectively reduced in *MIR205HG*-null animals but not miR-205 knock-in mutant mice. A. Serum prolactin levels were measured by ELISA using serum obtained from 5–6-week old mice. The mice included C57BL/6 controls (Ctl), *MIR205HG*$^{-/-}$ and littermate controls, and miR-205$^{-/-}$ animals with female and male designations indicated. In the case of nursing dams, samples were drawn at 8–10-days post parturition. B. RNA was isolated from the skin, thymus, and pituitary tissue of 4-week old female mice using control C57BL/6, *MIR205HG*-null, and miR-205-deficient lines. Quantitative miR-205 RT-PCR was performed as in Figure 2B and the relative expression calculated by $\Delta\Delta C_T$ normalized to 5S RNA. Data are representative of mean +/− SEM from at least 3 mice per group. *p<0.05, **p<0.01, ***p<0.001, ****p<0.0001 (students t-test

and two-way ANOVA). C. CRISPR/Cas genome targeting was used to create a miR-205-knock-in line. The DNA repair template of the pre-mature mmu-miR-205 sequence targeted the key bases that define the seed sequence specificity of miR-205. The nucleotide changes are indicated in green. D. The body weight, and *Zbtb20*, *prolactin*, and *growth hormone* transcript levels were compared among miR-205$^{KI/KI}$ mice versus their littermate controls. The transcript levels were determined as described in Figure 3D.

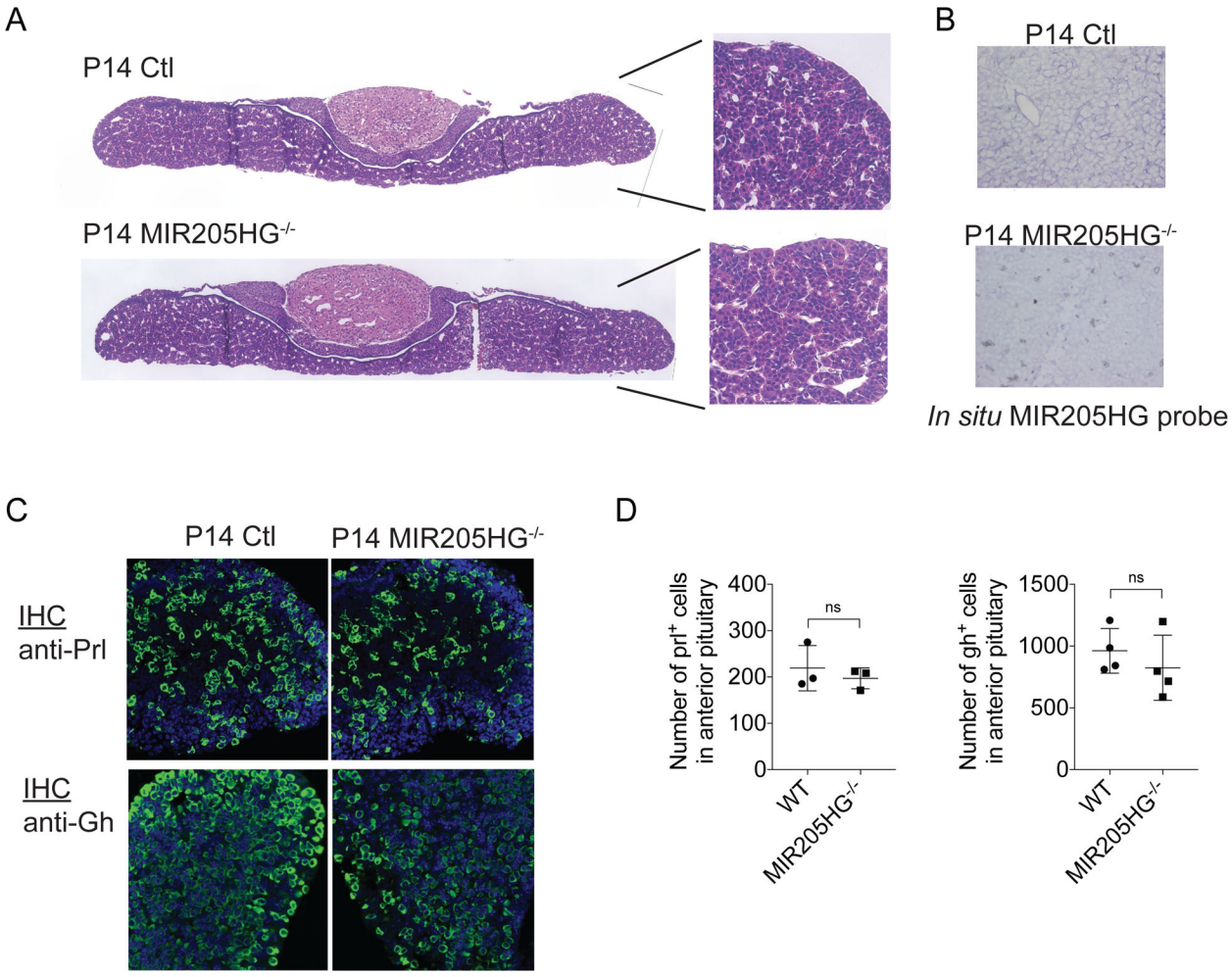

Figure 5.

Somatotrope and lactotrope cell lineages are maintained in the anterior pituitary in the absence of *MIR205HG*. A. The pituitary tissues from control and *MIR205HG*$^{-/-}$ P14 mice were processed for H&E staining. Sections comprising the entire pituitary and a segment of the anterior pituitary from P14 mice are shown. B. *In situ* hybridization with a *MIR205HG* specific antisense probe was undertaken with the pituitary from control and *MIR205HG*-null animals. C. Immunofluorescence imaging was performed with pituitary tissues isolated from 14-day old pups (P14) using age-matched controls or *MIR205HG* deficient mice. Prolactin- and growth hormone producing cells were stained with antibodies specific for each hormone (detected with Alexa Fluo 488 labelled 2° antibodies). Cell nuclei were stained with DAPI. D. The number of cells staining positive for growth hormone and prolactin was enumerated in the indicated mice. Data represent an analysis using a minimum of 3 control and 3 *MIR205HG*-null animals. P values are indicated for those with significant differences (students t-test and two-way ANOVA). ns indicates no significant difference.

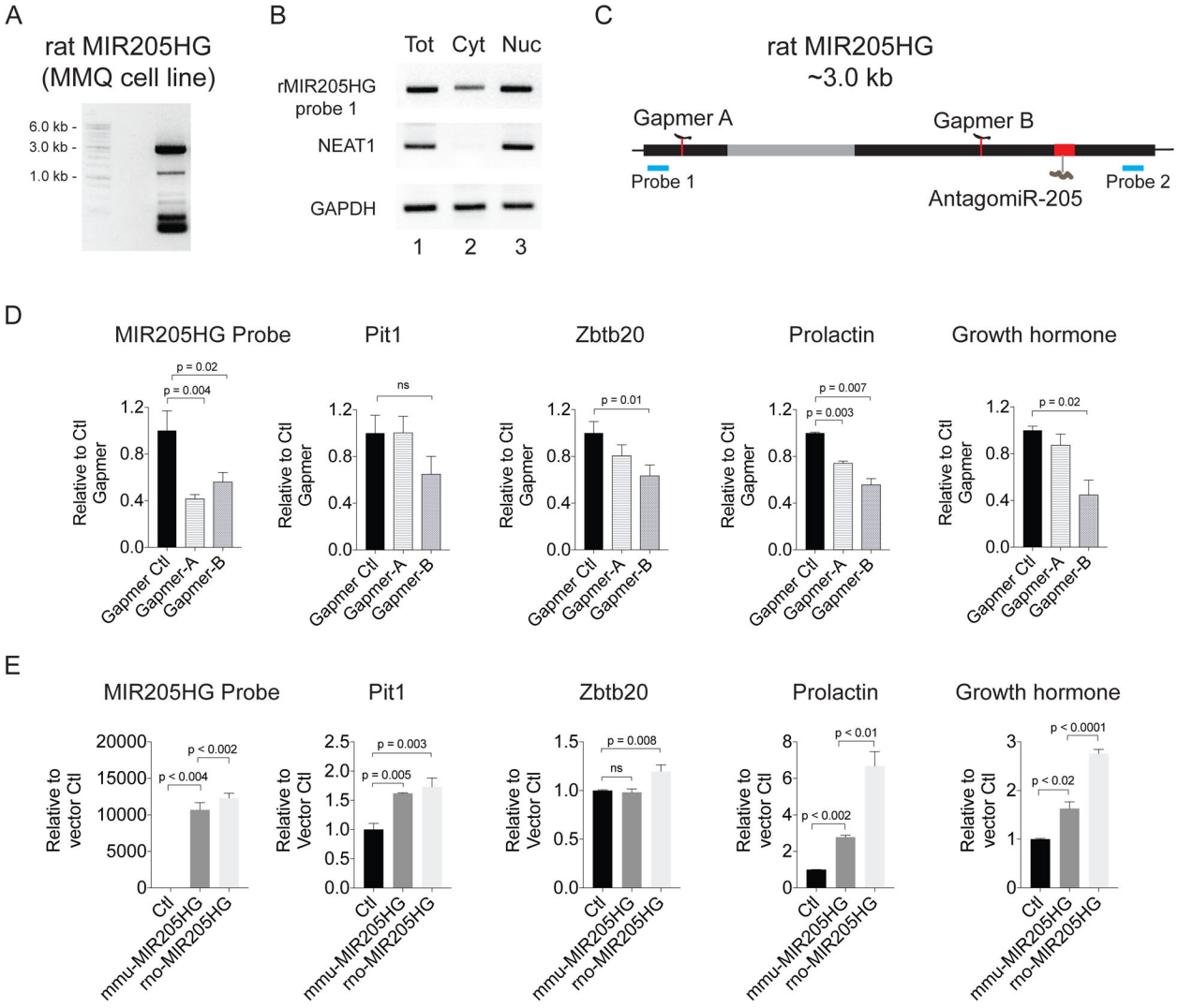

Figure 6.

MIR205HG positively regulates prolactin and growth hormone in a rat lactotrope cell line. A. MMQ, a rat lactotrope cell line, was used to isolate RNA for RT-PCR reactions with primers specific for rat *MIR205HG*. Multiple-sized transcripts are present, much like that seen with mouse tissues. B. RNA was extracted from cytoplasmic and nuclear extracts of the MMQ cells. This was used for RT-PCR with primers specific for rat *MIR205HG* and *NEAT*, the latter a lncRNA restricted to the nucleus. Control reactions were performed with Gapdh specific primers. C. Schematic of the rat *MIR205HG* exon assembly. Locked nucleic acid (LNA™) GapmeRs were designed to target the proximal and distal regions of the lncRNA (GapmeR A and B). The various control and rat *MIR205HG* specific GapmeRs are listed in Supplemental Table 3. The location of the antagomir specific for miR-205 is also shown. D. Control and *MIR205HG*-specific GapmeRs were introduced into the MMQ cell line. Forty-eight hrs. post-transfection, RNA was isolated and qRT-PCR reactions with rat specific primers used to compare the levels of *MIR205HG* (Probe 2), *Pit1*, *Zbtb20*, *prolactin*, and *growth hormone*. The relative expression of the indicated transcripts is shown after normalization to control GapmeR treated cells. E. Control lentiviral expression vectors

or those containing either murine or rat *MIR205HG* were used to over-express the lncRNA in MMQ cells. The levels of the indicated transcripts were determined as in (D). Data are representative of mean +/− SEM using at least two independent experiments (students t-test and two-way ANOVA).

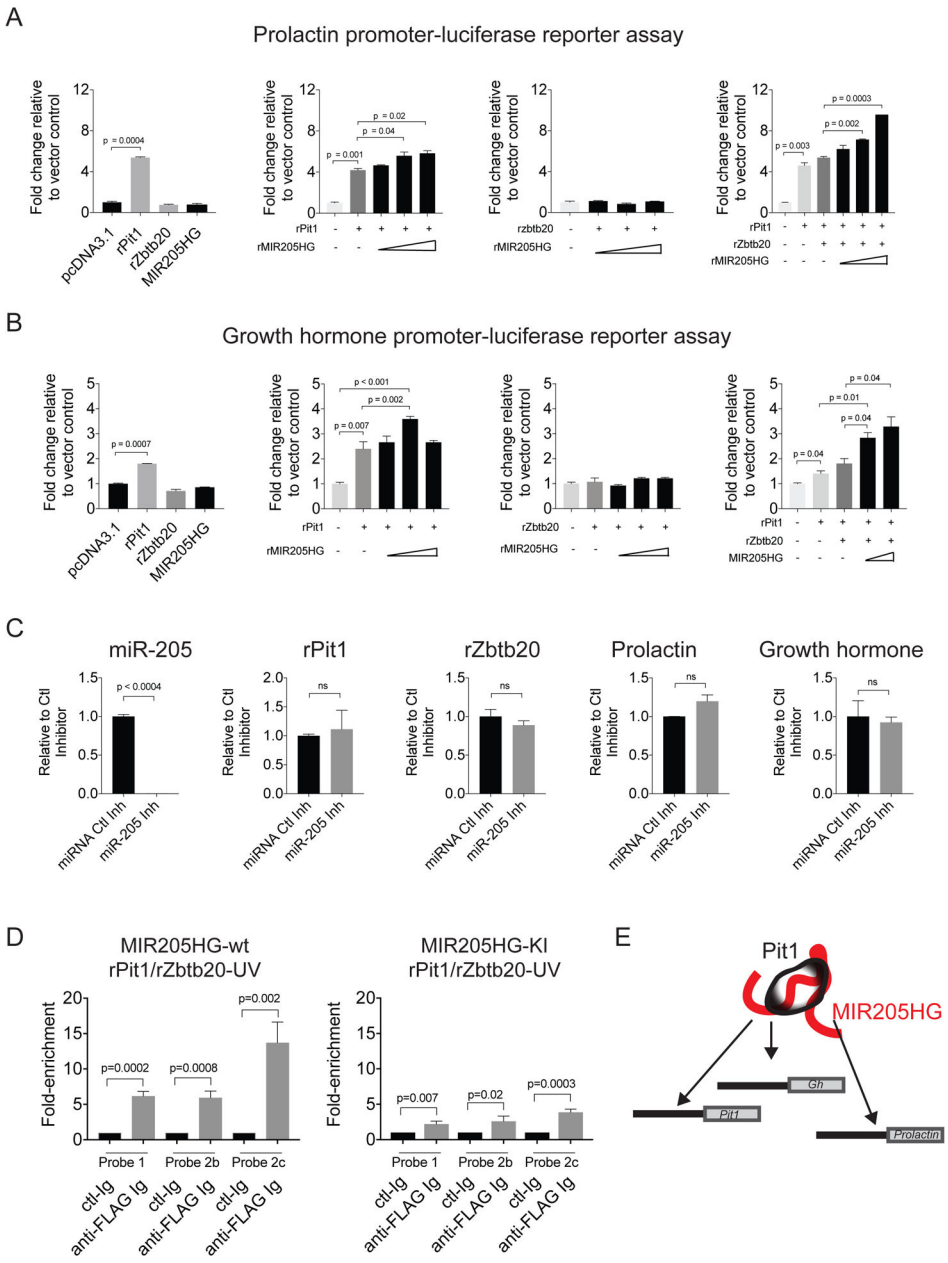

Figure 7.

MIR205HG regulates *Pit1*/*Zbtb2*0 transcriptional activity independent of miR-205. A. Luciferase reporter assays were performed using the prolactin promoter cloned upstream of luciferase. Transient transfection assays were performed in HEK293T cells with plasmids containing the rat prolactin-luciferase reporter construct with/without expression constructs for rat *Pit1*, *Zbtb2*0, and rat *MIR205HG*, the latter added in a dose-dependent manner. Data are representative of two independent experiments with p values calculated using student t-tests. B. The luciferase reporter assays were performed as in A. using the growth hormone promoter cloned upstream of luciferase. Data are representative of two independent experiments with p values calculated using student t-tests. C. MMQ cells were incubated with a control inhibitor or one specifically targeting miR-205 (antagomir). The levels of

miR-205 were determined 48 hrs post antagomir addition using quantitative miRNA-RT-PCR. Primers specific for rat *Pit1*, *Zbtb20*, prolactin, and growth hormone were used for regular qRT-PCR. Significance was determined by t-tests with differences that were not significant listed as ns. D. HEK293T cells were transfected with either wild-type or the knock-in mutation in miR-205 in the full-length MIR205HG construct. These cells were also transfected with rat *Pit1* and rat *Zbtb20*. Forty-eight hrs post-transfection, the cells were UV-cross-linked, lysed, and control IgG or anti-FLAG IgG immunoprecipitations undertaken. The precipitates were washed, proteinase K treatment, and RNA isolated. The RNA was used for qRT-PCR reactions with probes for human gapdh, murine MIR205HG targeting exon 1 (Probe 1, primers 1403/1406), exon 2b (Probe 2, primers 945/946) and exon 2c (Probe 3, primers 1194/1195), the latter detecting transcripts distal to miR-205. Results are obtained from two independent experiments, performed with triplicate samples. Statistical significance was determined by Student t-tests and is shown.

KEY RESOURCES TABLE

REAGENT or RESOURCE	SOURCE	IDENTIFIER
Antibodies		
Anti-murine growth hormone	NHPP	AFP564180Rb
Anti-murine prolactin	NHPP	AFP107120402R
Anti-Digoxigenin-AP	Roche	11093274910
Anti-CD8-FITC	Tonbo	35–0081-U500
Anti-CD4-PE	Tonbo	50–0041-U100
Anti-TCR-b-PerCP-Cy5.5	Tonbo	65–5961-U100
Anti-CD69-APC	ebioscience	17-0691-82
Anti-CD45-PerCPCy.5	biolegend	103132
Anti-B220-APC	Tonbo Sciences	20–0452-U100
Anti-CD44-APC	BD bioscience	559250
Anti-CD25-FITC	BD bioscience	553072
Anti-CD8-PE	Tonbo	50–0081-U100
Anti-B220-PE	BD bioscience	553090
Anti-NK1.1-PE	BD bioscience	553165
Anti-γδTCR-PE	BD bioscience	553178
Anti-CD11b-PE	BD bioscience	557397
Anti-CD11c-PE	Tonbo	50–0114-U100
Anti-CD19-PE	Tonbo	50–0193-U100
Anti-Ter-119-PE	Tonbo	50–5921-U100
Anti-CD62L-PE	BD bioscience	553151
Anti-CD4-PE-Cy5	BD bioscience	553654
Anti-FLAG mAb	Sigma Chemical	F1804
Anti-gapdh	Santa Cruz	47724
Bacterial and Virus Strains		
XL1-Blue Supercompetent Cells	Agilent	200236
BL21-Codon PLus	Agilent	230280
DH5 alpha	Invitrogen (ThermoFisher)	18265017
Biological Samples		
Embryos	C57BL/6 mice	
Thymus	C57BL/6 mice	
Skin	C57BL/6 mice	
Pituitary	C57BL/6 mice	
Hypothalamus	C57BL/6 mice	
Liver	C57BL/6 mice	
Bladder	C57BL/6 mice	
Tails	C57BL/6 mice	

REAGENT or RESOURCE	SOURCE	IDENTIFIER
Chemicals, Peptides, and Recombinant Proteins		
polyinosinic-polycytidylic acid (polyI:C)	Sigma Chemical	P1350
Turbo DNAase	Invitrogen-Fisher	AM2238
Critical Commercial Assays		
Mouse prolactin ELISA Kit	Thermo Fisher	EMPRL
Corticosterone ELISA Kit	Arbor Assays	K014-H1
Rat/Mouse Growth Hormone	EMD Millipore	EZRMGH-45K
Luciferase Assay System	Promega	E1500
MEGAscript™ T7 Transcription Kit	Invitrogen	AM1334
High Capacity cDNA synthesis kit	ABI-Thermo Fisher	4368814
miRCURY LNA RT Kit	Qiagen	339340
FluoReporter™ lacZ/Galactosidase Quantitation Kit	Thermo Fisher	F2905
Magnachip ProteinA/G magnetic beads	EMD Millipore	16–663
Deposited Data		
GEO Affymetrix Identifier	Mouse Clariom S	GES126943
Experimental Models: Cell Lines		
MMQ	ATCC	CRL-10609
HEK 293T	ATCC	CRL-3216
NIH3t3	ATCC	CRL-1658
OP9-Dll1 (stromal feeder cell line)	Juan Carlos Zuniga-Pflucker	
TEC427.1(thymic epithelial cell line)	Stanislas Vukmanovic	
J774A.1 (macrophage)	ATCC	TIB-67
DC2.4 (dendritic cell)	Sigma-Aldrich	SCC142
Experimental Models: Organisms/Strains		
C57BL/6	The Jackson Laboratory	#000664
MIR205HG$^{floxed/floxed}$ and KO	UTSW Transgenic Core Facility	Clone 4H11
miR_205$^{floxed/floxed}$	Mouse mutant resource center	MGI:2676880
miR-205$^{KI/KI}$	UTSW Transgenic Core Facility	B8 and B12 Lines
CAG-Cre	Rhonda-Bassel Duby UT Southwestern	Sakai and Miyazaki, 1997
Flpo-Cre	Mouse mutant resource center	MGI:4415609
Foxn1-Cre	The Jackson Laboratory	#018448
Oligonucleotides		
RT-PCR Primers, cloning primers	IDT, Exiqon (Qiagen)	Tables S2–S3
miR-205 LNA inhibitor	Qiagen	Table S3
MIR205HG GapmeR	Qiagen	Table S3
MIR205HG KI sgRNA	IDT DNA Technologies	Table S2

REAGENT or RESOURCE	SOURCE	IDENTIFIER
Recombinant DNA		
pCDNA3.1	Thermo Fisher	V79020
pCDNA3.1 mouse MIR205HG	van Oers Lab	#839
pCDNA3.1 mouse MIR205HG-KI	van Oers lab	#840
pCDNA3.1 rat MIR205HG	van Oers Lab	#841
pCDNA3.1 rat zbtb20	van Oers Lab	#843
pCDNA3.1 rat Pit-1	van Oers Lab	#842
pGL4.30[luc2P/NFAT-RE/Hygro]	Promega	E8481
pGL4.30[luc2P/ rPrl.1.7kb]	van Oers Lab	#850
pGL4.30[luc2P/rGH.promoter]	van Oers Lab	#866
pGEM-T easy vector system	Promega	A1360
pGEM-MIR205HG probe	van Oers Lab	N/A
pBluescript-Foxn1	van Oers Lab	N/A
pBluescript-Gcm2	van Oers Lab	N/A
pBluescript-Pitx2	van Oers Lab	N/A
pCDH-CMV	Addgene	#72265
pCDH-CMV-rat MIR205HG	van Oers lab	#854
pCDH-CMV-mouse MIR205HG	van Oers lab	#852
pCDH-CMV-mouse MIR205HG KI	van Oers lab	#853
Software and Algorithms		
SnapGene	GSL Biotech LLC	
Graphpad Prism	Prism 7 for MAC	
Flowjo	FlowJo LLC	
Other		